Swirling Cavity Flow of Water through a Straight Circular Pipe II

Toshihiko IKEDA* and Michio OHJI**

(Received May 31, 1972)

1. Introduction

As regards the flow structure of a swirling cavity flow of water, Hashimoto[1] proposed a triple structure model consisting of a free vortex, a forced vortex and a cavity. In the recent experiments of the present authors[2], however, the swirling velocity profile around a cavity was found to be of different nature, and this result may be attributed to an effect of the upstream conditions.

In this part of papers, an attempt is made to show some theoretical predictions on a simplified model system in which the swirl generator is replaced with a circular coaxial gap. There are two points in this study; the effect of the upstream conditions on the downstream flow, and the determination of the cavity radius. At the present stage, the theory is merely a preliminary one, direct comparison with experimental data being not intended here. Unless particularly stated, symbols in the previous paper[2] (referred to as I hereafter) will be used here as before.

2. Analytical procedures

Consider a steady axisymmetric swirling flow of an inviscid fluid, for which we have

$$\frac{\partial^2\psi}{\partial r^2}-\frac{1}{r}\frac{\partial\psi}{\partial r}+\frac{\partial^2\psi}{\partial z^2}=r^2\frac{dH}{d\psi}-\Gamma\frac{d\Gamma}{d\psi}, \tag{1}$$

where $\psi(r, z)$ denotes Stokes' stream function, $H(\psi)=\frac{1}{2}(v_r^2+v_\theta^2+v_z^2)+\frac{p}{\rho}$ Bernoulli's function and $\Gamma(\psi)=rv_\theta$ is the circulation. See Appendix (A10).

As a simplest model of the experimental setup, the swirl generator is replaced with a circular coaxial gap of the effective cross-sectional area $\pi(R^2-r_0^2)$ in

* Research Associate, Department of Mechanical Engineering.
** Professor, Department of Mechanical Engineering.

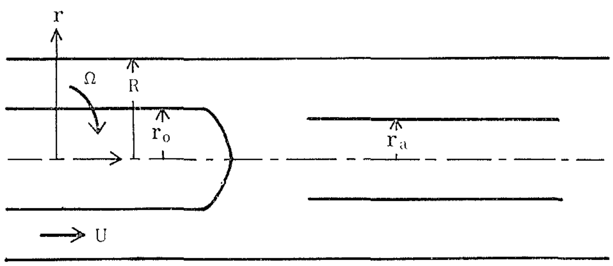

Fig. 1 A model of a swirling cavity flow of water through a straight circular pipe

which the water has a uniform axial velocity U and rotates as a rigid body with angular velocity Ω (Fig. 1).

Thus the theory described in Appendix is applicable, and the problem is to find such a downstream solution of Eq. (1) that the static pressure is equal to the *prescribed* cavity pressure p_a at a certain radius $r = r_a$(cavity wall). If the variation in hydrostatic pressure is neglected, the solution would be independent of z as $z \to \infty$, and can be written as

$$\psi(r) = \frac{1}{2}Ur^2 + rF(r), \tag{2}$$

$$v_\theta = \Omega r + n_0 F(r), \tag{3}$$

$$v_z = U + n_0 G(r), \tag{4}$$

where

$$\left.\begin{aligned} F(r) &= AJ_1(n_0 r) + BY_1(n_0 r) \\ G(r) &= AJ_0(n_0 r) + BY_0(n_0 r) \end{aligned}\right\}; \quad n_0 = 2\Omega/U \tag{5}$$

J's and Y's being Bessel functions of the first and second kind, and A, B the integral constants. See Appendix (A16) and (A17). Putting $a_0 = a = R$, $b_0 = r_0$, $b = r_a$ in (A18), we have here

$$\left.\begin{aligned} A &= \frac{U}{2r_a} \frac{(r_0^2 - r_a^2)\, Y_1(n_0 R)}{J_1(n_0 R)\, Y_1(n_0 r_a) - J_1(n_0 r_a)\, Y_1(n_0 R)}, \\ B &= \frac{-U}{2r_a} \frac{(r_0^2 - r_a^2)\, J_1(n_0 R)}{J_1(n_0 R)\, Y_1(n_0 r_a) - J_1(n_0 r_a)\, Y_1(n_0 R)}. \end{aligned}\right\} \tag{6}$$

In these expressions the cavity radius r_a is left as a disposable parameter to be determined in the following way:

First, from the balance of forces in the r-direction, the upstream pressure is given by

$$\frac{p(r)}{\rho}=\frac{P_0}{\rho}-\frac{\Omega^2}{2}(R^2-r^2), \tag{7}$$

where P_0 is the upstream wall pressure at $r=R$. The corresponding stream function and Bernoulli's function are

$$\psi=\frac{1}{2}Ur^2, \tag{8}$$

$$H(\psi)=\frac{1}{2}U^2+\frac{2\Omega^2}{U}\psi+\frac{P_0}{\rho}-\frac{\Omega^2R^2}{2}, \tag{9}$$

which yield

$$H_1=\frac{1}{2}U^2+\frac{\Omega^2R^2}{2}+\frac{P_0}{\rho}\quad\text{at the outer wall }(\psi=\psi_1=\frac{1}{2}UR^2), \tag{10}$$

and

$$H_2=\frac{1}{2}U^2+\Omega_2r_0^2+\frac{P_0}{\rho}-\frac{\Omega^2R^2}{2}\quad\text{at the inner wall }(\psi=\psi_2=\frac{1}{2}Ur_0^2), \tag{11}$$

respectively. Since the two streamlines $\psi=\psi_1$ and $\psi=\psi_2$ are still on the boundaries in the downstream region, the wall pressure p_w and the cavity pressure p_a are found to be

$$\frac{p_w}{\rho}=H_1-\frac{1}{2}(v_{\theta1}^2+v_{z1}^2)=\frac{P_0}{\rho}+\frac{1}{2}[U^2+\Omega^2R^2-(v_{\theta1}^2+v_{z1}^2)], \tag{12}$$

and

$$\frac{p_a}{\rho}=H_2-\frac{1}{2}(v_{\theta2}^2+v_{z2}^2)=\frac{P_0}{\rho}+\frac{1}{2}[U^2+\Omega^2(2r_a^2-R^2)-(v_{\theta2}^2+v_{z2}^2)], \tag{13}$$

where $v_{\theta1}$, v_{z1} are the velocity components at $r=R$ and $v_{\theta2}$, v_{z2} are those at $r=r_a$.

This last equation (13) determines the cavity radius r_a for a given set of parameters R, r_0, U, Ω, P_0 and p_a. With this value of r_a the appropriate downstream velocity profiles are obtained from Eqs. (3) to (6).

The downstream pressure distribution can be found from the balance of forces in the r-direction again. In virtue of Eqs. (3) and (5), and with the aid of indefinite integral formulas[4],

$$\left.\begin{aligned}\int\frac{J_1^2(x)}{x}dx &= -\frac{1}{2}[J_0^2(x)+J_1^2(x)],\\ \int\frac{J_1(x)Y_1(x)}{x}dx &= -\frac{1}{2}[J_0(x)Y_0(x)+J_1(x)Y_1(x)],\\ \int\frac{Y_1^2(x)}{x}dx &= -\frac{1}{2}[Y_0^2(x)+Y_1^2(x)],\end{aligned}\right\}\tag{14}$$

the result is that

$$\frac{p(r)}{\rho}=\int\frac{v_\theta^2}{r}dr+\text{const.}=\frac{1}{2}\Omega^2r^2-2\Omega G-\frac{n_0^2}{2}(F^2+G^2)+\text{const.}\tag{15}$$

This can be rewritten as

$$\frac{p(r)}{\rho}=\frac{P_0}{\rho}+\frac{1}{2}(U^2-\Omega^2R^2)+\Omega rv_\theta-\frac{1}{2}(v_\theta^2+v_z^2),\tag{16}$$

which reduces to (12) and (13) at $r=R$ and r_a respectively. We may also use the relations (9), (2) and (3) to get the same expression as (16).

3. Non-dimensional form

By introducing the non-dimensional quantities

$$r_0/R=\alpha,\ \ r_a/R=\beta,\ \ n_0R=\frac{2\Omega R}{U}=\gamma_0,\ \ r/R=\eta,\tag{17}$$

the foregoing results are expressed in a non-dimensional form as

$$\frac{v_\theta(\eta)}{U}=\frac{\gamma_0}{2}[\eta+\lambda f(\eta)],\ \ \frac{v_z(\eta)}{U}=1+\frac{\gamma_0}{2}\lambda g(\eta),\tag{18}$$

and

$$\frac{p(\eta)-P_0}{\frac{1}{2}\rho U^2}=-\frac{\gamma_0^2}{4}[(1-\eta^2)+\lambda^2\{f^2(\eta)+g^2(\eta)\}]-\gamma_0\lambda g(\eta)\tag{19}$$

where

$$\lambda=\frac{\alpha^2-\beta^2}{\beta f(\beta)},\tag{20}$$

$$f(\eta)=Y_1(\gamma_0)J_1(\gamma_0\eta)-J_1(\gamma_0)Y_1(\gamma_0\eta),\tag{21}$$

$$g(\eta) = Y_1(\gamma_0) J_0(\gamma_0 \eta) - J_1(\gamma_0) Y_0(\gamma_0 \eta). \tag{22}$$

For comparison with experiments it is convenient to rewrite these in terms of the downstream quantities. In view of the continuity relation, the mean axial velocity at the downstream section $\bar{v}_z$ is given by

$$\bar{v}_z(1-\beta^2) = U(1-\alpha^2) = U\sigma_0, \text{ i. e., } \bar{v}_z = U\sigma, \tag{23}^*$$

The downstream swirl ratio then becomes

$$\gamma = 2v_{\theta 1}/\bar{v}_z = \frac{1}{\sigma}\gamma_0, \tag{24}$$

and hence we have

$$\frac{v_\theta(\eta)}{\bar{v}_z} = \frac{\gamma}{2}[\eta + \lambda f(\eta)], \quad \frac{v_z(\eta)}{\bar{v}_z} = \frac{1}{\sigma} + \frac{\gamma}{2}\lambda g(\eta), \tag{25}$$

and

$$k_s(\eta) = \frac{p(\eta) - p_w}{\frac{1}{2}\rho(\bar{v}_z{}^2 + v_{\theta 1}{}^2)} = \frac{\frac{\gamma^2}{4}}{1 + \frac{\gamma^2}{4}}[(\eta^2 - 1) + \lambda^2\{g_1{}^2 - f^2(\eta) - g^2(\eta)\}$$
$$+ \frac{\gamma}{\sigma}\lambda\{g_1 - g(\eta)\}], \tag{26}$$

where g_1 is the value of g at the wall ($\eta = 1$).

The procedure of finding the appropriate solution is thus as follows:

(i) For a given set of values of $\sigma_0(=1-\alpha^2)$ and γ_0, plot

$$p(\beta) = p_w + \frac{1}{2}\rho(\bar{v}_z{}^2 + v_{\theta 1}{}^2)k_s(\beta) \tag{27}$$

as a function of β.

(ii) A value of β such that $p(\beta) = p_a$ is the cavity radius for those values of (σ_0, γ_0).

(iii) With this value of β, compute the velocity and pressure distributions after (25) and (26).

4. Numerical examples and remarks

Calculations have been carried out for the values of parameters $\gamma_0 = 1, 2, 3,$

* Note that $\sigma_0 = 1 - \alpha^2$ and $\sigma = (1-\alpha^2)/(1-\beta^2)$ are the geometrical and actual area parameters, respectively. see I, Notation.

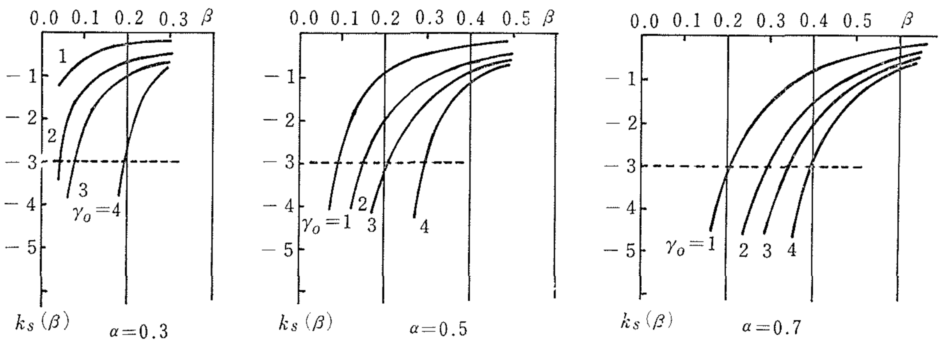

Fig. 2 The cavity condition $k_s(\beta)$ vs. cavity radius β

Table 1 Computed β and the other typical values

$k_s(\beta) = -3$

α	γ_0	β	σ	γ
0.7	1	0.21	0.53	1.87
	2	0.30	0.56	3.57
	3	0.35	0.58	5.16
	4	0.40	0.61	6.59
0.5	1	0.09	0.76	1.32
	2	0.15	0.77	2.61
	3	0.21	0.78	3.82
	4	0.29	0.82	4.89
0.3	1	—	—	—
	2	0.05	0.91	2.19
	3	0.08	0.92	3.28
	4	0.19	0.94	4.24

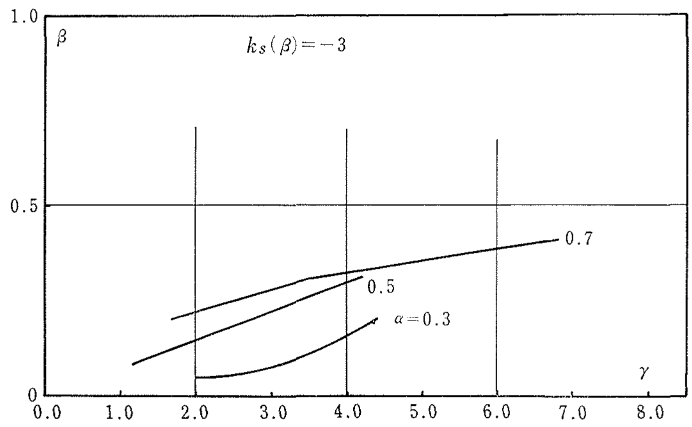

Fig. 3 The cavity radius β vs. downstream swirl ratio γ

4 and $\alpha = 0.3,\ 0.5,\ 0.7$ ($\sigma_0 = 0.91,\ 0.75,\ 0.51$, respectively). In Fig. 2 the function $k_s(\beta)$ is plotted for every combination of γ_0 and σ_0 (procedure (i) of the last section). However, the cavity radius β is determined here by the condition $k_s(\beta) = -3$ instead of the absolute pressure criterion $p(\beta) = p_a$ (procedure (ii)). This choice of critical value of $k_s(\beta)$ seems plausible in view of the previous experimental data I, and may suffice to see the general tendency of the solution.

Table 1 shows the computed values of important quantities, while Fig. 3 is a plot of the relation between γ and β. It is seen that β increases with γ in a rough qualitative agreement with experimental plot. (I; Fig. 4). The resemblance of the pressure and velocity distributions shown in Fig. 4 to experimental results (I; Figs. 5 to 18) is also only partial. Especially for strong swirl ($\gamma_0 = 4$), v_z is negative near the wall and v_θ has a maximum within the flow (Figs. 7, 11

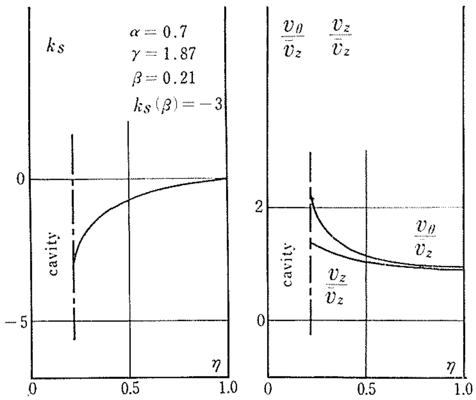

Fig. 4.

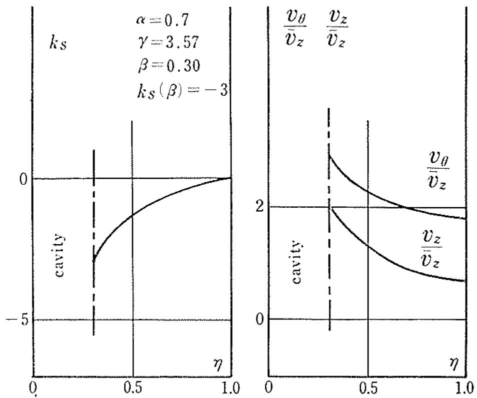

Fig. 5.

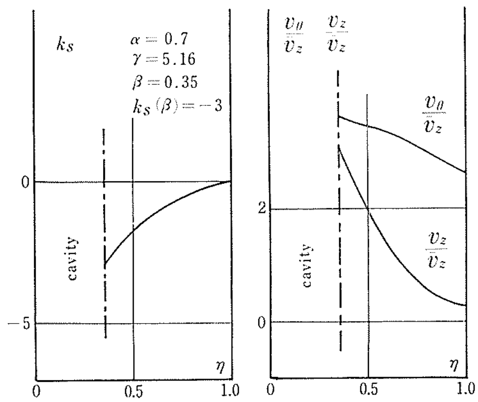

Fig. 6.

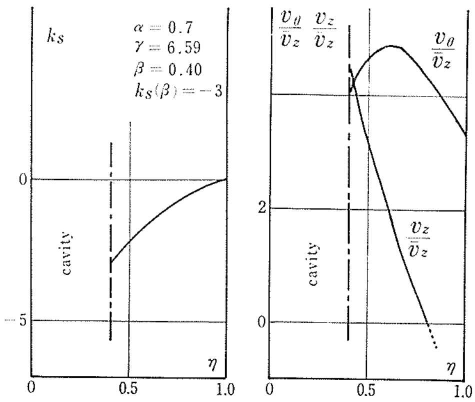

Fig. 7.

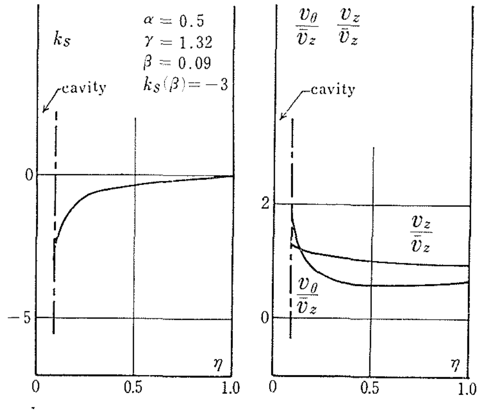

Fig. 8.

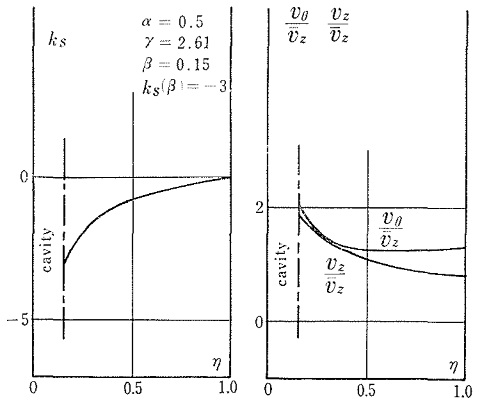

Fig. 9.

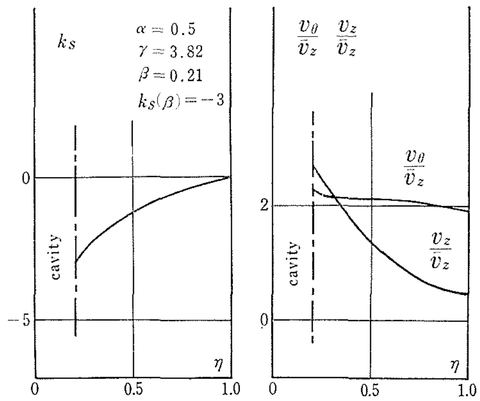

Fig. 10.

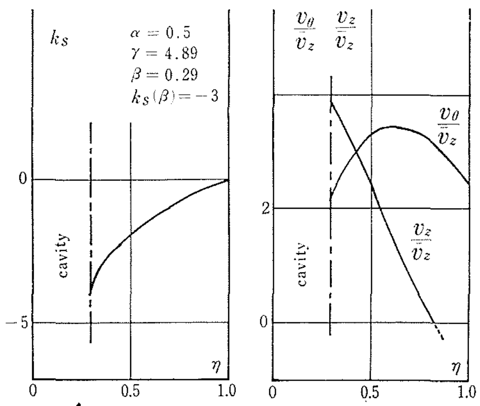

Fig. 11.

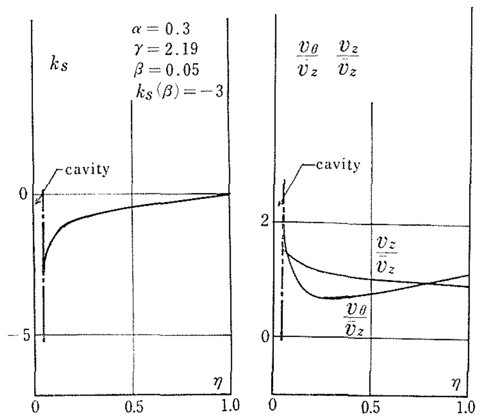

Fig. 12.

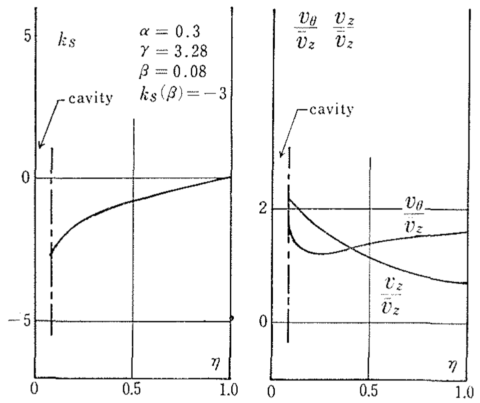

Fig. 13.

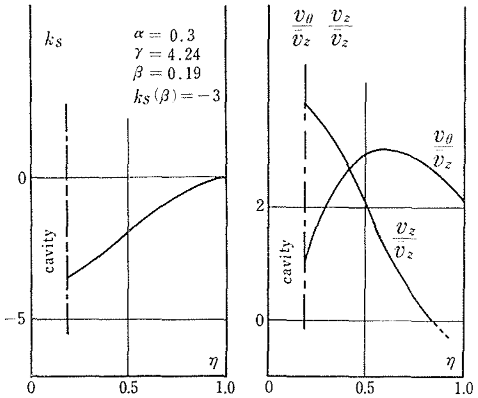

Fig. 14.

and 14). In such cases we have to replace the present analysis with a different kind of approach. See the footnote in Appendix. Another draw-back is that the theory predicts a finite cavity radius however γ is small, and a sharp peak of v_θ near the cavity for weak swirl ($\gamma_0 = 1$) is also unnatural. These diffiiculties will probably be remedied by a viscous theory. Lastly it should be noted that there is no experimental confirmation yet of the upstream condition of a rigid body rotation.

Appendix

An elegant and clear account of the theory of steady axisymmetric flow with swirl is given by Batchelor[3]. For convenience we shall recapitulate the argument briefly bellow.

Let $(v_r,\ v_\theta,\ v_z)$ and $(\omega_r,\ \omega_\theta,\ \omega_z)$ denote the velocity and vorticity components, respectively, in cylindrical coordinates $(r,\ \theta,\ z)$. The relevant equations of motion and mass-conservation for an inviscid incompressible fluid are expressed as

$$v_\theta \omega_z - v_z \omega_\theta = \partial H/\partial r, \tag{A1}$$

$$v_z \omega_r - v_r \omega_z = 0, \tag{A2}$$

$$v_r \omega_\theta - v_\theta \omega_r = \partial H/\partial z, \tag{A3}$$

$$v_r = -\frac{1}{r}\frac{\partial \psi}{\partial z}, \quad v_z = \frac{1}{r}\frac{\partial \psi}{\partial r}, \tag{A4}$$

where $H(r,\ z)$ is Bernoulli's function and $\psi(r,\ z)$ Stokes' stream function. Further we have immediately

$$\frac{1}{2}(v_r^2 + v_\theta^2 + v_z^2) + \frac{p}{\rho} = H(\psi) \tag{A5}$$

as well as

$$r v_\theta = \Gamma(\psi) \tag{A6}$$

since H and the circulation Γ are conserved along each streamline $\psi =$ const. which coincides with the path of a material element in steady flow. It follows then

$$\left.\begin{aligned} \omega_r &\equiv -\frac{1}{r}\frac{\partial \Gamma}{\partial z} = v_r \frac{d\Gamma}{d\psi}, \\ \omega_z &\equiv \frac{1}{r}\frac{\partial \Gamma}{\partial r} = v_z \frac{d\Gamma}{d\psi}, \end{aligned}\right\} \tag{A7}$$

in view of (A4), whereas

$$\omega_\theta \equiv \frac{\partial v_r}{\partial z} - \frac{\partial v_z}{\partial r} = -\frac{1}{r}\left(\frac{\partial^2 \psi}{\partial r^2} - \frac{1}{r}\frac{\partial \psi}{\partial r} + \frac{\partial^2 \psi}{\partial z^2}\right) \tag{A8}$$

by definition. Another relation obtained from either of Eqs. (A1) or (A3) is

$$\omega_\theta = \frac{\Gamma}{r}\frac{d\Gamma}{d\psi} - r\frac{dH}{d\psi}, \tag{A9}$$

and equating these two expressions for ω_θ, we get

$$\frac{\partial^2 \psi}{\partial r^2} - \frac{1}{r}\frac{\partial \psi}{\partial r} + \frac{\partial^2 \psi}{\partial z^2} = r^2\frac{dH}{d\psi} - \Gamma\frac{d\Gamma}{d\psi} \tag{A10}$$

This equation determines the stream function so long as H and Γ are known functions of ψ.

We shall now consider a steady swirling flow between two coaxial circular cylinders as shown in Fig. A1. If the fluid far upstream has uniform axial velocity U and rotates as a rigid body with angular velocity Ω, the corresponding stream function is $\psi_0 = Ur^2/2$, and hence we can write

$$\Gamma_0 = \frac{2\Omega}{U}\psi_0, \quad H_0 = \frac{1}{2}U^2 + \frac{2\Omega^2}{U}\psi_0 + \text{const.}, \tag{A11}$$

where the suffix 0 refers to upstream conditions. Since the dependences (A11)

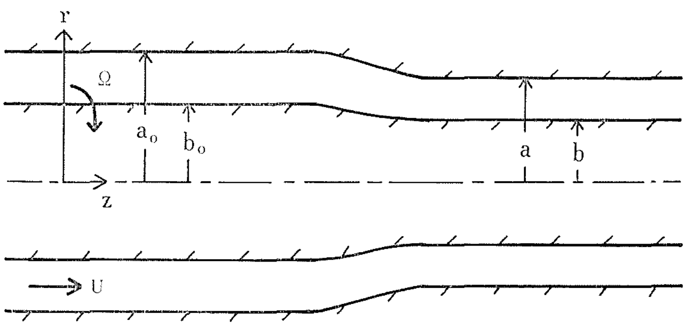

Fig. A1 General model.

should hold over the whole field*, we may drop the suffix to obtain

$$\frac{\partial^2\psi}{\partial r^2}-\frac{1}{r}\frac{\partial\psi}{\partial r}+\frac{\partial^2\psi}{\partial z^2}=\frac{2\Omega^2}{U}r^2-\frac{4\Omega^2}{U^2}\psi, \tag{A12}$$

for the equation (A10). This reduces to a simpler form

$$\frac{\partial^2 F}{\partial r^2}+\frac{1}{r}\frac{\partial F}{\partial r}+\frac{\partial^2 F}{\partial z^2}+\left(n_0^2-\frac{1}{r^2}\right)F=0, \tag{A13}$$

by putting

$$\psi(r,\ z)=\frac{1}{2}Ur^2+rF(r,\ z) \quad \text{and} \quad n_0=2\Omega/U. \tag{A14}$$

As $z\to\infty$, the flow becomes independent of z again, and we are concerned with Bessel's equation

$$\frac{d^2F}{dr^2}+\frac{1}{r}\frac{dF}{dr}+\left(n_0^2-\frac{1}{r^2}\right)F=0, \tag{A15}$$

which gives

$$F(r)=AJ_1(n_0r)+BY_1(n_0r), \tag{A16}$$

and accordingly

$$\left.\begin{aligned} v_\theta &= \Gamma/r=\Omega r+n_0[AJ_1(n_0r)+BY_1(n_0r)], \\ v_z &= \frac{1}{r}\frac{d\varphi}{dr}=U+n_0[AJ_0(n_0r)+BY_0(n_0r)], \end{aligned}\right\} \tag{A17}$$

in turn.

In order to determine the constants A and B, we have only to notice that the streamlines $\psi=Ua_0^2/2$ and $\psi=Ub_0^2/2$ far upstream are still on the outer and inner walls respectively far downstream. The result is

$$\left.\begin{aligned} A &= \frac{U}{2ab}\frac{b(a_0^2-a^2)Y_1(n_0b)-a(b_0^2-b^2)Y_1(n_0a)}{J_1(n_0a)Y_1(n_0b)-J_1(n_0b)Y_1(n_0a)}, \\ B &= -\frac{U}{2ab}\frac{b(a_0^2-a^2)J_1(n_0b)-a(b_0^2-b^2)J_1(n_0a)}{J_1(n_0a)Y_1(n_0b)-J_1(n_0b)Y_1(n_0a)}. \end{aligned}\right\} \tag{A18}$$

* This statement is not the case, if there appears a reverse flow which comes from the downstream region. In such a case we cannot proceed beyond the equation (A10), and hence the solution (A16) together with (A17), (A18) cease to be valid.

Reference

1) H. HASHIMOTO, "Swirling flow accompanied by cavity in circular tube", *Rep. Inst. High Speed Mech., Japan,* Vol. 19 (1967–1968), pp. 241–257.

2) T. IKEDA and M. OHJI, "Swirling cavity flow of water through a straight circular pipe I" *J. Faculty of Engineering Shinshu University, Japan,* No. 32 (1972), pp. 1–9.

3) G. K. BATCHELOR, "An introduction to fluid dynamics", *Cambridge University Press* (1967).

4) W. JAHNKE and F. EMDE, "Tables of functions with formulas and curves", *Dover Publ., New York* (1945).